

# The Effect of Cross-sectional Area of The Microwave Argon Discharge Tube on Some Plasma Parameters using COMSOL Multiphysics

Noor H. Ali<sup>1\*</sup> and Mohammed R. Abdulameer<sup>1</sup>

<sup>1</sup>*Department of Physics, College of Science, University of Baghdad, Baghdad, Iraq*

\*Corresponding author: [Nour.Hameed1704b@sc.uobaghdad.edu.iq](mailto:Nour.Hameed1704b@sc.uobaghdad.edu.iq)

## Abstract

Microwave plasma plays a vital role in various scientific and technological applications due to its high efficiency and flexibility. The geometry of the discharge tube, especially its cross-sectional area, significantly affects essential plasma parameters such as electron density, ion density, and electron temperature. These parameters directly influence plasma behaviour, including energy absorption and electromagnetic field distribution. This study employs COMSOL Multiphysics software to analyze how variations in the cross-sectional area of the discharge tube impact plasma characteristics. The objective is to identify patterns that could improve the design and performance of plasma-based systems, with potential benefits in fields like medical tissue purification, environmental applications, and manufacturing. The tube had a constant length of 25 cm and varying widths between 1 and 14 cm, resulting in cross-sectional areas from 25 to 350 cm<sup>2</sup>. The results revealed that increasing the area notably affects thermal stability, energy distribution, and plasma penetration. Electron density and temperature changed with the area; the highest electron density was  $2.05 \times 10^{18} \text{ m}^{-3}$  at 175 cm<sup>2</sup>. Electron temperature varied between 1.5 eV at 100 cm<sup>2</sup> and 1.75 eV at 25 cm<sup>2</sup>, peaking at 1.65 eV at 175 cm<sup>2</sup>.

## 1. Introduction

The efficiency, robustness, and versatility of microwave-generated plasma make it widely used in many scientific and industrial fields. The discharge tube, which acts as a gas ionization medium, is a major factor in determining the properties and behavior of these plasmas. The main plasma properties, such as electron density, ion density, and electron temperature, are significantly affected by the geometrical aspects of the microwave discharge cylindrical tube, especially its cross-sectional area [1,2]. A comprehensive understanding of these properties is important for optimizing plasma systems, which improve efficiency and effectiveness in various applications, including materials processing, environmental remediation, and medical sterilization. In microwave argon plasma discharges, the cross-section shape of the discharge tube and the electromagnetic-field distribution are important factors influencing energy absorption and the subsequent plasma formation processes like variations in cross sections [3,4].

This study used COMSOL Multiphysics software and finite difference method calculations to investigate the effect of varying the cross-sectional area of the microwave discharge tube on important plasma properties. This study examines various tube geometries to identify patterns and interactions that facilitate the design of efficient and high-quality plasma systems. The results of this work are expected to greatly improve the practical application of microwave plasma devices by providing valuable insights into the relationship between discharge tube geometry and plasma performance. These results will provide understanding and knowledge of plasma energy which has been enhanced, and laid the foundation for advanced plasma technology [5-7].

## Article Info.

### Keywords:

*Plasmas, Microwave, COMSOL, Argon Discharge, Microwave Discharge.*

### Article history:

*Received: Nov. 30, 2024*

*Revised: Feb. 27, 2025*

*Accepted: Apr 07, 2025*

*Published: Mar. 01, 2026*



## 2. Theoretical Background

### 2.1. Plasma and its Properties

Plasma, often called the fourth state of matter, is a highly energized gas made up of neutral particles, ions, and free electrons. In contrast to other states of matter, like solid, liquid, and gas, plasma displays distinctive characteristics, including electrical conductivity, composition, and electrochemical properties [8]. As a result, plasma is important in many commercial and scientific applications. Electron density, ion density, electron temperature and plasma frequency are the parameters that define the physicochemical properties of plasma and govern its behaviour. These properties are important in the interaction of plasma with the environment and have effective roles in various fields [9].

Microwave plasma is a specific type of plasma generated by electromagnetic radiation in the 2.45 GHz microwave frequency band. This plasma is ideal for applications where plasma properties need to be accurately configured due to low ionic strength and high electron density. These applications include environmental preparation, surface modification and thin film deposition, where specific plasma properties are necessary to achieve the desired results [10].

### 2.2. Role of Discharge Tube Geometry in Plasma Behavior

In a microwave plasma system, the discharge tube is the physical chamber where gas ionization and plasma generation occur. The geometry of the tube, especially its cross-sectional area, greatly influences the properties of the plasma. It affects important plasma properties, such as cohesion, ionization efficiency, and energy absorption, by affecting the potential density, electromagnetic dispersion, and charged particles in the cavity [11]. With small cross-sectional area, the power density, the electron temperature and ionization rate can be made high. In contrast, a large cross-sectional area tends to distribute electromagnetic energy over a wider area and can decrease temperature and electron density, promoting more uniform plasma formation. Tube geometry and plasma dynamics can maximize plasma performance, ensuring energy efficiency and achieving acceptable plasma characteristics for specific applications and thorough analysis of the complex essential connections [12].

### 2.3. Microwave Argon Discharge

Argon is commonly used in plasma systems due to its low ionization energy, inert nature, and stable plasma generation. Energy absorbed in a microwave field ionizes air in microwave argon discharges, generating plasma with improved electron density and customizable properties. The microwave energy distribution is greatly affected by the cross-sectional area of the discharge tube. Therefore, how the ionization effectively works determines the properties of the resulting plasma, such as electron density, cohesion, and stability [13,14].

### 2.4. Simulation of Plasma Behavior Using COMSOL Multiphysics

The main method for investigating plasma dynamics is to simulate plasma systems using computer tools such as COMSOL Multiphysics [15,16]. COMSOL is an excellent tool for measuring the effects of geometrical changes in the drainage system while facilitating the description of coupled electromagnetic plasma dynamics [17,18]. This study used the COMSOL Multiphysics plasma module to evaluate the effects of variations in the cross-sectional area of the discharge tube on some important plasma properties, including electron temperature, electron density, and ionization rate [19,20]. These examples elucidate the basic principles governing plasma behavior in geometrical systems [21].

## 2.5. Relevance of the Study

Understanding the effect of the discharge tube cross-sectional area on plasma properties is vital to improve microwave plasma equipment performance. Accurate plasma properties protocols are essential for applications such as surface treatment, thin film deposition, and plasma-enhanced chemical processing [22]. This ensures that changes in plasma properties, such as temperature, cohesion, and electron density, match the specific requirements of each application [23]. This work seeks to reconcile theoretical predictions with actual experiments by providing a better understanding of how discharge tube geometry affects plasma behavior. The results of this research will facilitate the creation and operationalization of microwave plasma systems well and versatile [24].

## 2.6. Model Definition

The electron and average electron energies are obtained by solving two drift diffusion equations [25]

$$\frac{\partial}{\partial t}(n_e) + \nabla \cdot [-n_e(\mu_e \cdot \mathbf{E}) - \mathbf{D}_e \cdot \nabla n_e] = R_e \quad (1)$$

$$\frac{\partial}{\partial t}(n_\varepsilon) + \nabla \cdot [-n_\varepsilon(\mu_\varepsilon \cdot \mathbf{E}) - \mathbf{D}_\varepsilon \cdot \nabla n_\varepsilon] + \mathbf{E} \cdot \Gamma_e = R_\varepsilon \quad (2)$$

where  $n_e$  is the electron density,  $\mathbf{D}_e$  is the electron diffusion,  $n_\varepsilon$  is the energy density, and  $\mathbf{D}_\varepsilon$  is the energy diffusion.

The electron source  $R_s$  and the energy loss from inelastic collisions  $R_\varepsilon$  are specified. Electron diffusivity, energy mobility, and energy diffusivity are derived from electron mobility by the following equations

$$\mathbf{D}_e = \mu_e T_e, \mu_\varepsilon = \left(\frac{5}{3}\right) \mu_e, \mathbf{D}_\varepsilon = \mu_\varepsilon T_e \quad (3)$$

Using rate coefficients, plasma chemistry determines the source coefficients in the aforementioned equations. The electron source term for rate coefficients is [25]

$$R_e = \sum_{j=1}^M x_j k_j N_n n_e \quad (4)$$

where  $x_j$  represents the mole fraction of the target species for reaction  $j$ ,  $k_j$  denotes the rate coefficient for reaction  $j$  (in SI unit of  $\text{m}^3/\text{s}$ ), and  $N_n$  signifies the total neutral number density (in SI unit of  $1/\text{m}^3$ ). The electron energy loss is calculated by aggregating the collisional energy loss across all processes

$$R_\varepsilon = \sum_{j=1}^P x_j k_j N_n n_e \Delta \varepsilon_j \quad (5)$$

where  $\Delta \varepsilon_j$  is the energy loss from reaction  $j$ . The rate coefficients can be computed from cross section data by the following integral

$$k_k = \gamma \int_0^\infty \varepsilon \sigma_k(\varepsilon) f(\varepsilon) d\varepsilon \quad (6)$$

where  $\gamma = (2q/m_e)^{1/2}$  (in SI unit of  $\text{C}^{1/2}/\text{kg}^{1/2}$ ),  $m_e$  is the electron mass,  $\varepsilon$  is energy,  $\sigma_k$  is the collision cross section, and  $f$  is the electron energy distribution function. In this case, a Maxwellian EEDF is assumed.

In a microwave reactor the high frequency electric field is computed in the frequency domain using the following equation [25]

$$\nabla \times (\mu_r^{-1} \nabla \times \mathbf{E}) - k_0^2 \left( \epsilon_r - \frac{j\sigma}{\omega \epsilon_0} \right) \mathbf{E} = 0 \quad (7)$$

with a DC magnetic field present, the electric field-plasma current density connection gets knottier. An equation describing this connection is as follows

$$\sigma^{-1} \cdot \mathbf{J} = \mathbf{E} \quad (8)$$

where  $\sigma$  is the plasma conductivity tensor, which is a function of the electron density, collision frequency, and magnetic flux density. Using the definitions [25]

$$\alpha = \frac{q}{m_e(v_e + j\omega)}, \beta = n_e q \alpha \quad (9)$$

where  $q$  represents the charge of the electron,  $m_e$  denotes the mass of the electron,  $n_e$  indicates the frequency of collisions, and signifies the angular frequency of the electromagnetic field. In the absence of an external DC magnetic field, the inverse of the plasma conductivity here is represented in a diagonal form

$$\sigma^{-1} = \begin{bmatrix} \frac{1}{\beta} & 0 & 0 \\ 0 & \frac{1}{\beta} & 0 \\ 0 & 0 & \frac{1}{\beta} \end{bmatrix} \quad (10)$$

The gas flow is represented with the premise of a steady speed in the x-direction [25].

## 2.6. Plasma Chemistry

The chemical process of plasma comprises three species and seven reactions, including electron impact cross-sections essential for sustaining low-pressure argon discharges, such as elastic scattering, excitation, superelastic ionization, Penning ionization (the process where two metastable argon atoms combine to yield a neutral argon atom, an argon ion, and an electron), and metastable quenching. Superelastic collisions with electrons, deactivation by neutral argon atoms, ionization, or Penning ionization reduce the presence of excited argon atoms. The gas is activated by heat as a result of metastable quenching. As the excited metastable state deteriorates, the 11.5 eV of energy used to create the electrically excited argon atom is released into the surroundings as heat. Surface reactions have volumetric reactions. The sticking coefficient quantifies the likelihood that a metastable argon atom will transit to a ground state argon atom upon colliding with the wall [25].

## 3. Results and Discussion

### 3.1. Work Procedure

Changing the cross-sectional area of an Ar gas discharge tube when the absorbed power ( $P_0$ ) is constant at 100W, the following steps was done:

- 1- Go to model builder
- 2- From the global definition option and parameter1.
- 3- From the settings window, we fix the value  $p_0=100w$ .
- 4- We change the cross-sectional area of the gas tube in two dimensions by going to

Component1→Rectangle2 (r2), from the properties setting window in the size and shape box, we fix the width at 25cm and the height, we change it according to the required area from 25 to 350cm<sup>2</sup> and an increase of 25 cm<sup>2</sup>.

5- Press the compute button.

6- We also go to the results box in the model builder and click on the plasma variables such as electron density (plas) 1 and electron temperature (plas) 1. electric potential (plas) 1 and electric field (emw) 1.

7- The results will appear in the form of graphs on the right side of the program and we will save them on the laptop to discuss and analyze them later.

The absorbed power from the waveguide was in the TE mode and maintained at  $P_0=100\text{W}$ . The cross-sectional area of the discharge tube was rectangular in shape, with a fixed length of 25 cm and different widths from 1 to 14 cm. The area(A) of the discharge tube was varied from 25 to 300 cm<sup>2</sup> in increments of 25 cm<sup>2</sup>. This was conducted to investigate the influence of the area on the properties and variables of plasma generated by the microwave discharge, including electron temperature and density, electric field, and potential.

### 3.2. Microwave system Description

In this basic microwave apparatus, the microwave at a frequency of 2.45 GHz is sent from the base of the plasma discharge tube through a waveguide, where it interacts with the Ar flowing gas, under a pressure of 1 Torr, leading to its heating and ionization and the formation of plasma, as seen in Fig.1.

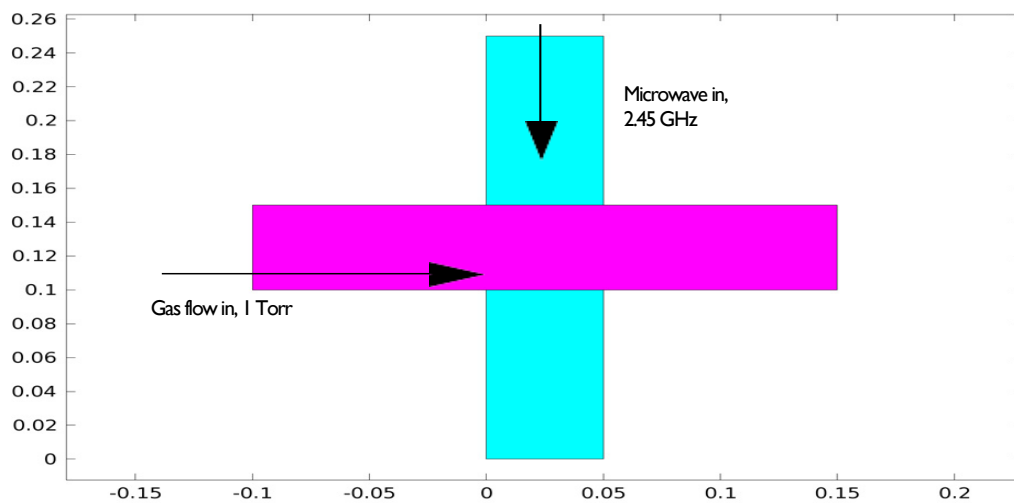


**Figure 1: Diagram of a geometric structure of the discharge system. Microwave comes in from the top port and interacts with the gas flow, resulting in the creation of plasma [23].**

### 3.3. Electron Density ( $n_e$ )

Fig.2 represents the spatial distribution of the density of electrons when increasing the cross-sectional area (A) of the discharge tube from (25-150 cm<sup>2</sup>).

In Fig.2(a), for the area  $A = 25 \text{ cm}^2$ , it is observed that the electron density concentration in the center of the discharge tube decreases progressively as moving away from the center. Specifically, the electron density at the center of the discharge was  $7 \times 10^{17} \text{ m}^{-3}$ . At a distance of 7.5 cm from the center along the negative x-axis, the density was approximately  $2 \times 10^{17} \text{ m}^{-3}$ . Furthermore, at the tube walls on the positive x-axis side, 25 cm from the center, the electron density was measured to be  $4 \times 10^{17} \text{ m}^{-3}$ . The electron density distribution at the center was represented as a contour, specifically resembling a concentric ellipse. The reduction in electron density as one moves away from the center

can be attributed to the migration of electrons from regions of high pressure to those of low pressure. The peak electron density at the center resulted from direct exposure to the microwave source, which enhanced ionization and consequently increased the ionization ratio, increasing electron density. Fig.2(b) illustrates the absence of low-density electron regions observed in the preceding figure, with the electron gradient concentrated solely at the center of the tube. This phenomenon is attributed to the increase in cross-sectional area; in the prior figure, where the area was 25 cm<sup>2</sup>, electrons were densely packed within a limited space. Analysis of the Figs. 3-4 reveals that the electron density at the center exhibited an elliptical shape, which became less flattened as the area increased.

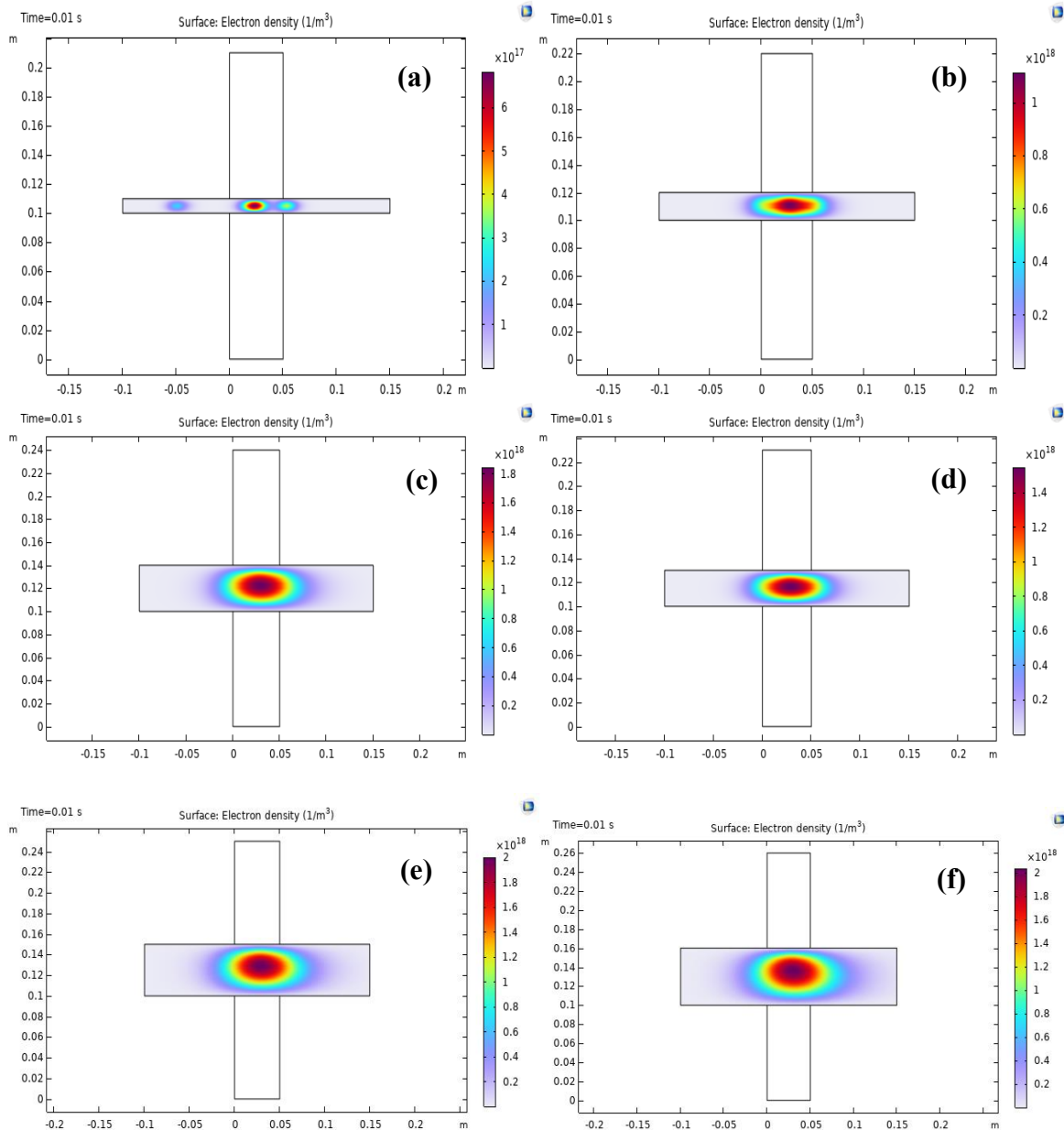


**Figure 2: Electron density spatial distributions at a fixed microwave absorbed power  $P_0$  of 100 W when A: (a) 25, (b) 50, (c) 75, (d) 100, (e) 125, and (f) 150 cm.<sup>2</sup>**

Additionally, the electron density at the center increased with the cross-sectional area of the discharge tube, reaching a limit of A=200 cm<sup>2</sup>. In Fig.2(f), when the value of A was 150 cm<sup>2</sup>, the electron density exhibited an almost circular shape. In Fig.4(m), when the area was adjusted to 325 cm<sup>2</sup>, it was observed that the electron density was low, ranging from (2-4) x 10<sup>17</sup> m<sup>-3</sup>, particularly at the boundaries and edges of the tube. This

phenomenon results from the increased area, which facilitates greater electron propagation, aligning with the findings presented in the COMSOL multiphysics user’s manual [22]. As indicated in Table 1, a larger cross-sectional area of the discharge tube correlates with a tendency for the electron density shapes to approach circularity.

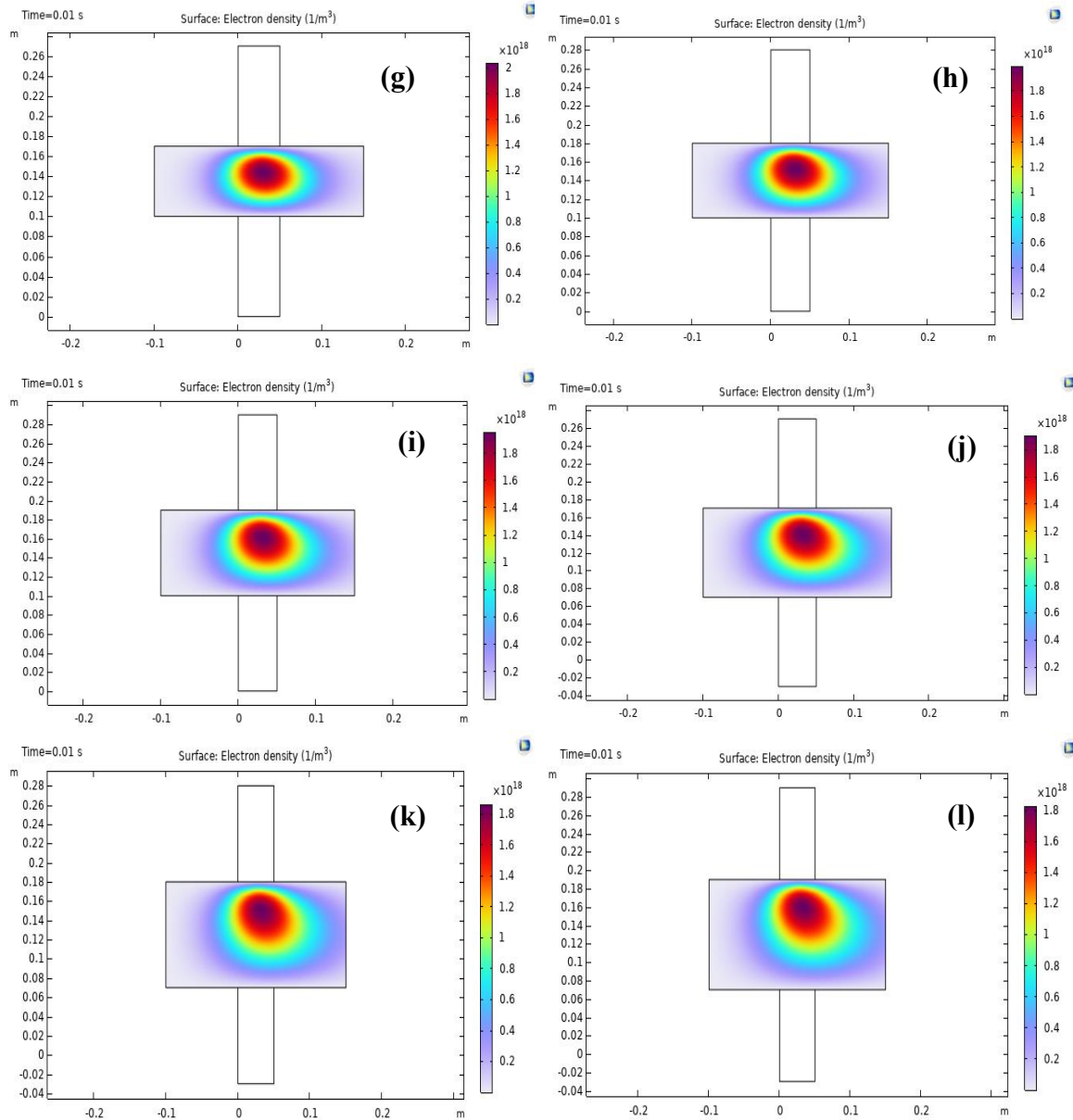


**Figure 3: Electron density spatial distributions at a fixed microwave absorbed power  $P_0$  when (A): (g) 75, (h) 200, (i) 225, (j) 250, (k) 275, and (l) 300 cm<sup>2</sup>**

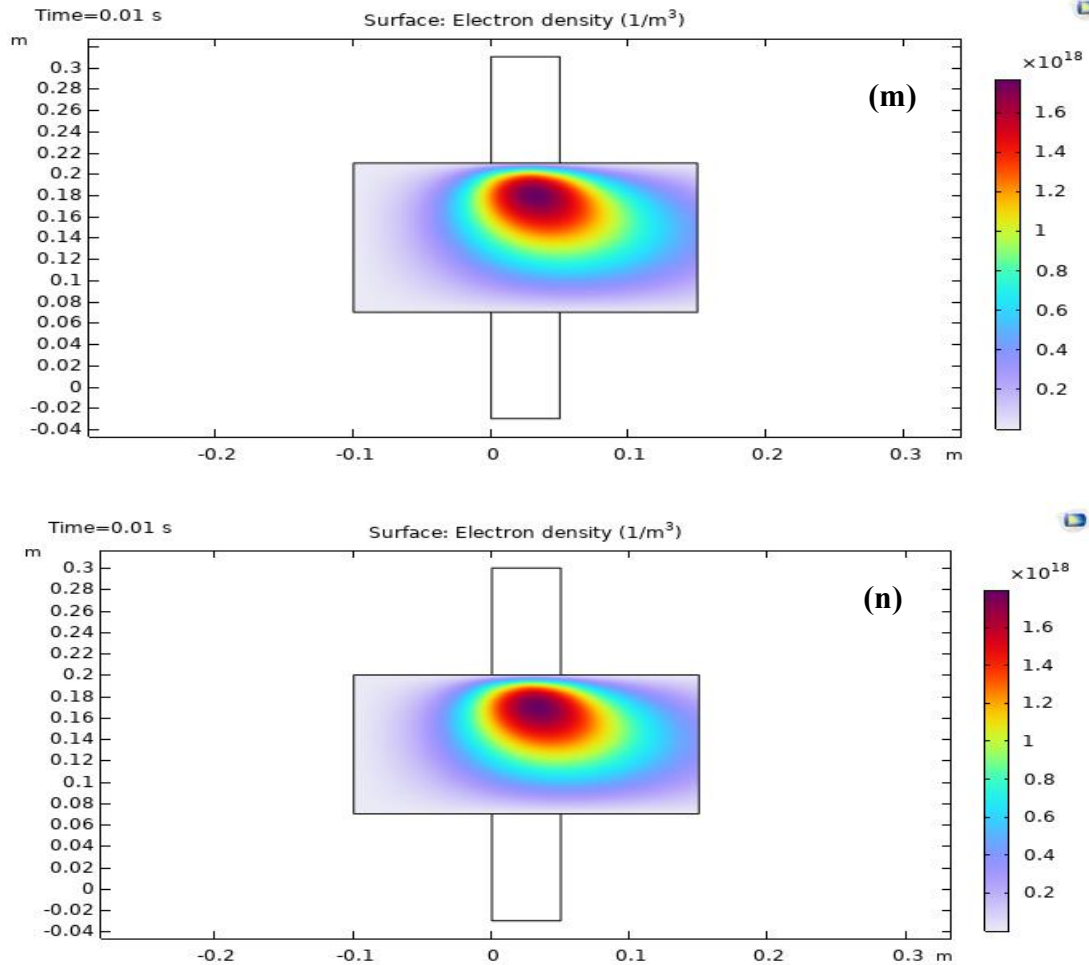


Figure 4: Electron density spatial distributions at a fixed microwave absorbed power  $P_0$  of 100 W when (A): (m) 325, and (n) 350  $\text{cm}^2$

Table 1: Variations of electron density and temperature against cross sectional area of Ar gas discharge tube (A) at a fixed microwave absorbed power  $P_0$  of 100 W.

A ( $\text{cm}^2$ )	$N_{e \text{ max}} (\text{m}^{-3}) \times 10^{17}$	$T_{e \text{ max}} (\text{eV})$
25	7	1.75
50	11	1.65
75	15	1.55
100	18	1.5
125	20	1.57
150	20.25	1.6
175	20.5	1.65
200	20	1.6
225	19.5	1.6
250	19	1.6
275	18.5	1.61
300	18	1.62
325	17.5	1.625
350	17	1.63

### 3.4. Electron Temperature ( $T_e$ )

Fig. 5 illustrates the spatial distribution of electron temperature within the discharge tube under a constant microwave absorbed power  $P_0$  of 100 W while varying the cross-sectional area of the tube. Fig.6 indicates a gradual decrease in temperature at the top of the cylindrical tube. The gas thermal equilibrium equation should be applied alongside

the equations of particle motion in quasi-isobaric conditions. The maximum value attained was 1.7 eV, as observed in Fig.6, where a decrease occurred, followed by a return to the peak value at the top of the tube wall. The tube wall typically served as the primary cooling mechanism for the gas, with the wall temperature provided as an input parameter. The axial distribution of the wall temperature was effectively modelled using a semi-empirical formula:  $T_w = T_0 + c(WR)\beta$  [1], where ( $T_0$ ) represents the room temperature in Kelvin (K),  $W$  denotes the specific discharge power in watt per cubic centimeter ( $\text{watt}/\text{cm}^3$ ), and ( $R$ ) indicates the tube radius in centimeters (cm), and ( $c$ ) and ( $\beta$ ) represent the relevant parameters, while  $WR$  denotes the total net energy transferred per unit volume to the transition states from the heat sources within the volume and the wall. Upon the abrupt cessation of the electromagnetic energy sustaining the discharge, the electrons will rapidly cool towards the final electron temperature value.

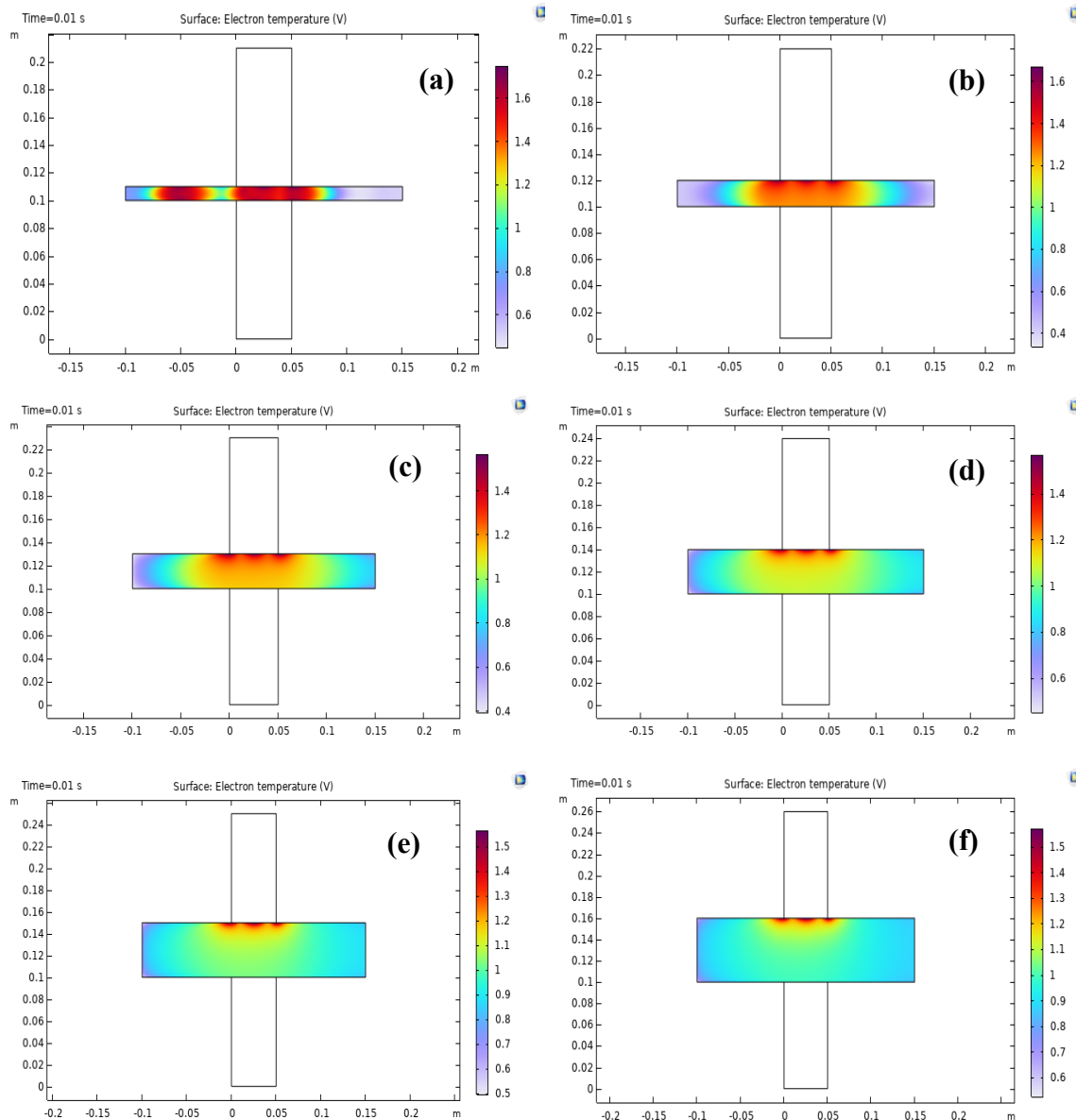


**Figure 5: Electron temperature spatial distributions at a fixed microwave absorbed power  $P_0$  of 100 W when (A): (a) 25, (b) 50, (c) 75, (d) 100, (e) 125, and (f) 150 $\text{cm}^2$ .**

Figs. 6-7 illustrate the impact of altering the cross-sectional area of the discharge tube on the electron temperatures within the produced plasma. The predominant pattern

seen is a drop in the electron temperature down to  $125 \text{ cm}^2$  with an increase in the cross-sectional area of the discharge cylinder, followed by a general increase until it reaches  $T_e = 1.63 \text{ eV}$  at an area of  $350 \text{ cm}^2$ . The increase is attributed to the acquisition of extra energy via ionization and collisions among charged particles, as well as between charged and neutral particles.

Fig. 8 depicts the fluctuation in electron density according to alterations in the cross-sectional area of the discharge tube, while maintaining a constant absorbed power in the argon gas microwave discharge plasma.

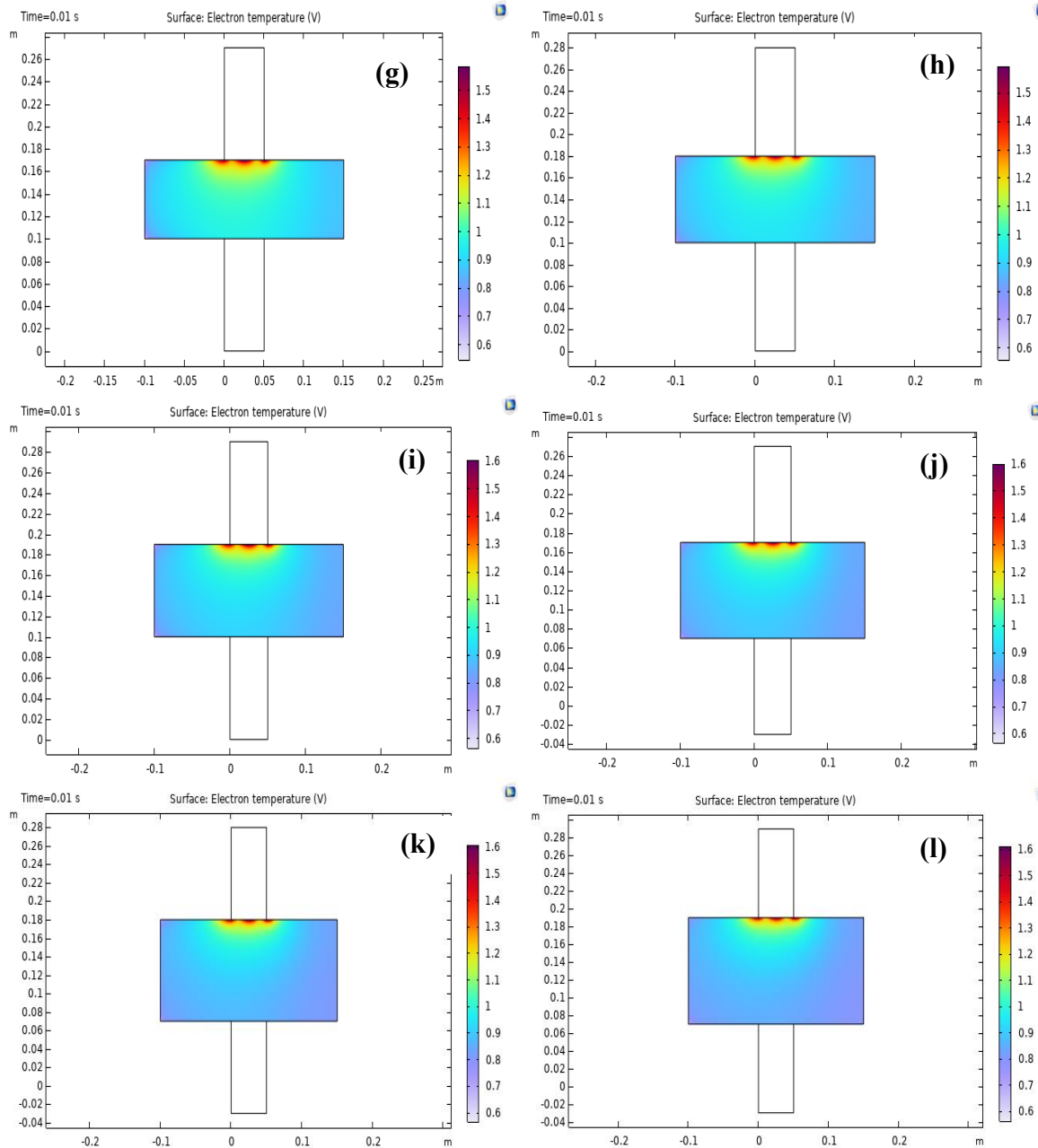


**Figure 6:** Electron temperature spatial distributions at a fixed microwave absorbed power  $P_0$  of 100 W when (A): (g) 175, (h) 200, (i) 225, (j) 250, (k) 275, and (l) 300  $\text{cm}^2$ .

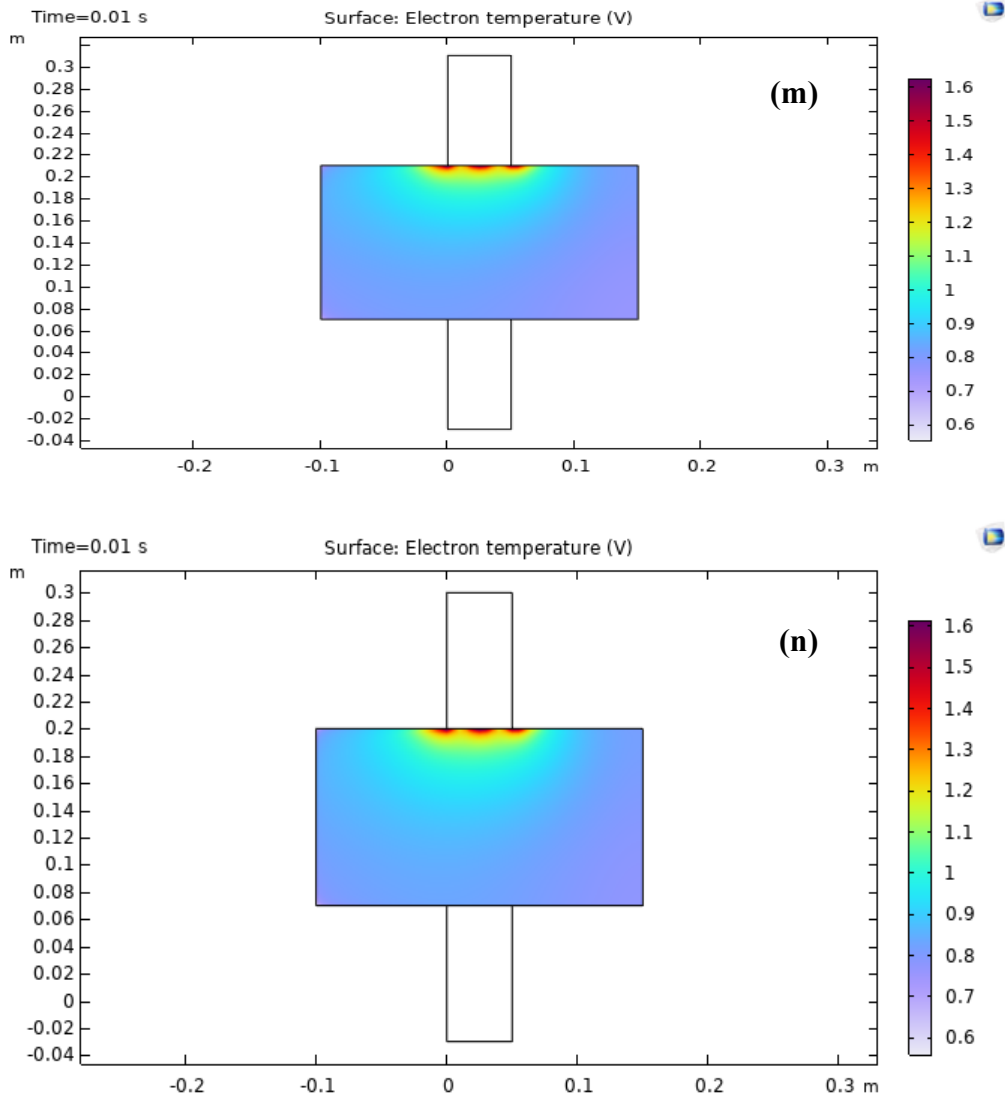


Figure7: Electron temperature spatial distributions at a fixed microwave absorbed power  $P_0$  of 100 W when (A): (m) 325, and (n) 350  $\text{cm}^2$ .

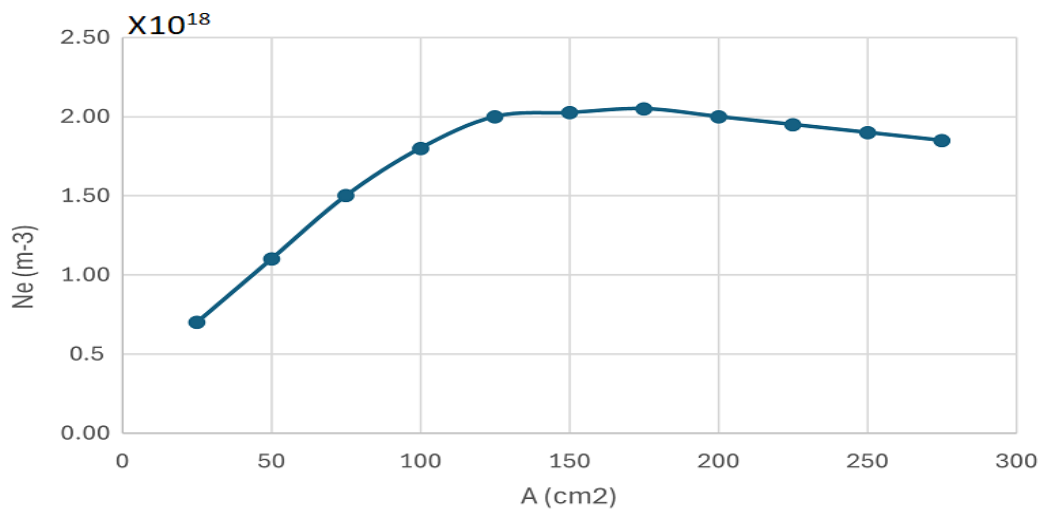
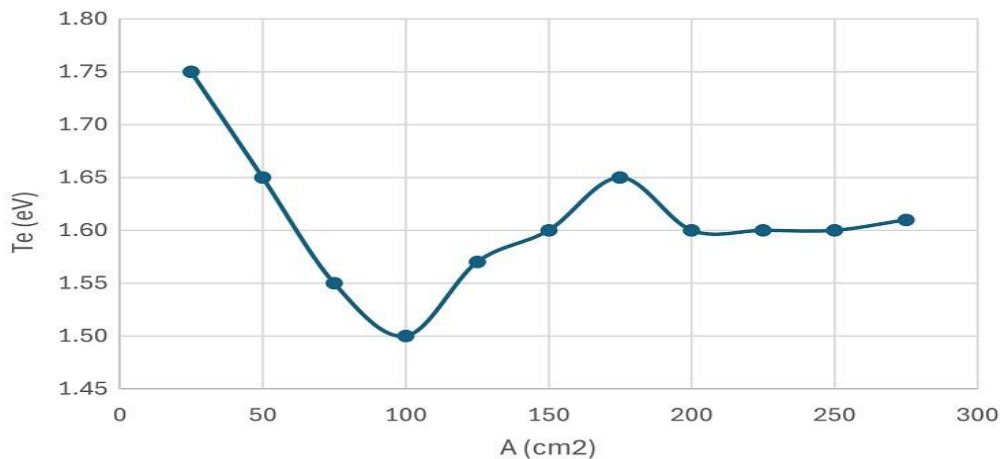


Figure 8: The effect of the cross-sectional area of the discharge tube on the electron density at a constant microwave absorbed power by the argon gas microwave discharge plasma particles.

As the cross-sectional area increases, the electron density increases from zero to an increase of  $2.3 \times 10^{18} \text{ m}^{-3}$ . These observations suggest that larger absorption areas of the plasma to the microwave lead to higher electron densities, possibly due to improved plasma confinement, and better energy absorption per unit volume. The observations suggest that an increase in sectional area increases the conditions for storing the electron population in a plasma to reach a certain ionization level. For plasma symmetry, the relationship between electrons density and cross-sectional area highlights the importance of discharge geometry influencing plasma properties, especially in applications such as microwave-driven plasma processes that require stable controlled electron density.

Fig. 9 shows the effect of the cross-sectional area of the discharge tube on the electron temperature at a constant microwave absorbed power.



**Figure 9:** The effect of the cross-sectional area of the discharge tube on the electron temperature when the power absorbed by the argon gas microwave discharge plasma particles is constant.

Initially, the electron temperature attains a maximum of 1.75 eV at a cross-sectional area of 25 cm<sup>2</sup>, although it exhibits a non-uniform trend with increasing cross-sectional area. Subsequent to the apex, the electron temperature diminishes till around 100 cm<sup>2</sup>, at this point it commences to increase once more. Beyond this threshold, from 200 to 300 cm<sup>2</sup>, the temperature becomes stable. The uneven pattern indicates that variations in cross-sectional area influence the energy distribution and confinement properties inside the plasma. The first temperature decline may stem from energy distribution over an expanded volume, but the following rise might signify an area of energy re-concentration, potentially due to spatial discrepancies in wave absorption. The stabilization phase presumably signifies a balanced energy distribution throughout the plasma cross-section, highlighting the critical role of discharge tube design in preserving electron temperature stability in designated areas.

#### 4. Conclusions

The findings illustrate the significant influence of the discharge tube's cross-sectional area on the plasma properties in microwave-induced argon discharges. Increased energy and particle concentration due to reduced cross-sectional areas elevate peak electron densities and temperatures. Larger regions, conversely, promote a more uniform distribution of energy, enhancing confinement and plasma uniformity. Material processing, ionization systems, and plasma-assisted technologies represent merely a fraction of the commercial and scientific applications where these insights are essential for enhancing the design and optimisation of plasma systems.

## Conflict of Interest

Authors declare that they have no conflict of interest.

## References

1. R. Gautam, S. Kumar, and S. Upadhyayula, *Renewable and Sustainable Energy Reviews*, **202**, 114735, (2024). <https://doi.org/10.1016/j.rser.2024.114735>.
2. S. Tiwari, A. Caiola, X. Bai, A. Lalsare, and J. Hu, *Plasma Chem. Plasma Process*, **40**, 1, (2020). <https://10.1007/s11090-019-10040-7>.
3. M. Hamidieh and M. Ghassemi, *IEEE Access*, **12**, 104688 (2024). <https://10.1109/ACCESS.2024.3435971>.
4. A. Ojha, H. Pandey, and S. Pandey, *IEEE Trans. Plasma Sci.*, **51**, 407, (2023). <https://10.1109/TPS.2023.3234079>.
5. M. Chaudhuri, A. V. Ivlev, S. A. Khrapak, H. M. Thomas, and G. E. Morfill, *Soft Matter*, **7**(4), 1287, (2011). <https://10.1039/C0SM00813C>.
6. M. Hori and B. A. Niemira, *J. Phys. D. Appl. Phys.*, **50**, 323001, (2017). <https://10.1088/1361-6463/aa76f5>.
7. S. Karunanithi, P. Guha, and P. P. Srivastav, *Food Bioprocess Technol.*, **16**(3), 603, (2023). <https://10.1007/s11947-022-02957-3>.
8. Y. A. Lebedev, *J. Phys. Conf. Ser.*, **257**, 012016, (2010). <https://10.1088/1742-6596/257/1/012016>.
9. G. J. Van Rooij, D. C. M. Van Den Bekerom, N. Den Harder, T. Minea, G. Berden, W. A. Bongers, R. Engeln, M. F. Graswinckel, E. Zoethouta, and M. C. M. Van De, *Sanden Faraday Discuss.*, **183**, 233, (2015). <https://10.1039/C5FD00045A>.
10. S. Rath and S. Kar, *Contrib. to Plasma Phys.*, **65**, 2 (2024). <https://10.1002/ctpp.202400036>.
11. K. Bouherine, A. Tibouche, N. Ikhlef, and O. Leroy, *IEEE Trans. Plasma Sci.*, **44**(12), 3409, (2016). <https://10.1109/TPS.2016.2619696>.
12. G. Chen, N. Britun, T. Godfroid, V. Georgieva, R. Snyders, and M. P. Delplancke-Ogletree, *J. Phys. D. Appl. Phys.*, **50**(8), 084001, (2017). <https://10.1088/1361-6463/aa5616>.
13. Y. A. Lebedev, *High Temp.*, **56**(5), 811, (2018). <https://10.1134/S0018151X18050280>.
14. M. J. H. Khan, Z. Kryzevicius, A. Senulis, A. Zukauskaitė, and P. Rapalis, *J. Uebe, Polym.*, **16**(21), 2990 (2024). <https://doi.org/10.3390/polym16212990>.
15. H. M. Abdulwahab and H. R. Humud, *Iraqi J. Sci.*, **65**, 151, (2024). <https://10.24996/ijs.2024.65.1.14>.
16. Y. Yamashita, R. Tsukizaki, K. Daiki, Y. Tani, R. Shirakawa, K. Hattori, and K. Nishiyama, *Acta Astronaut.*, **185**, 179, (2021). <https://10.1016/j.actaastro.2021.05.001>.
17. S. A. Khalaf and T. H. Khalaf, *Iraqi J. Sci.*, **65**, 175, (2024). [https://10.24996/ijs.\(2024\).65.1.16](https://10.24996/ijs.(2024).65.1.16).
18. K. A. Aadim, *Iraqi J. Phys.*, **15**(34), 138, (2019). <https://10.30723/ijp.v15i34.129>.
19. M. H. Jawad and M. R. Abdulameer, *Iraqi J. Sci.*, **64**, 1210, (2023). <https://10.24996/ijs.2023.64.3.17>.
20. H. H. Marza and Th. H. Khalaf, *Iraqi J. Phys.*, **20**(3), 98, (2022). <https://10.30723/ijp.v20i3.1017>.
21. T. Lin, H. Wang, T. Shen, Zhuoqun Deng, Ruifa Chai, Xinyuan Sun, Dongyuan Cui, Sai An, Wei Chen, and Yu-Fei Song, *Chimia (Aarau)*, **77**, 11, 733, (2023). <https://10.2533/chimia.2023.733>.
22. H. Y. Choi, Y. G. Park, and M. Y. Ha, *J. of Mechanical Sci. and Technol.*, **34**, 3303, (2020). <https://doi.org/10.1007/s12206-020-0722-2>.
23. A. A. Hussein and Th. H. Khalaf, *Iraqi J. Phys.*, **20**(4), 35, (2022). <https://10.30723/ijp.v20i4.1035>.
24. B. J. Xu, H. Wu, H. Z. Su, M. Y. Lee, Y. X. Zhang, Y. Chen, M. Liu, W.L. Wang, and Y. Du, *J. Clean. Prod.*, **436**, 140706, (2024). <https://10.1016/j.jclepro.2024.140706>.
25. A. Saifutdinov and E. Kustova, *Plasma Sources Sci. Technol.*, **32**(12), 125010, (2023). <https://10.1088/1361-6595/ad13a3>.

## تأثير مساحة المقطع العرضي لأنبوب تفريغ الأرجون بالميكروويف على بعض معاملات البلازما باستخدام فيزياء COMSOL Multiphysics

نور حميد علي<sup>1</sup> ومحمد رضا عبد الامير<sup>1</sup>  
<sup>1</sup>قسم الفيزياء، كلية العلوم، جامعة بغداد، بغداد، العراق

### الخلاصة

تعد بلازما الميكروويف مهمة في العديد من مجالات العلوم والتكنولوجيا نظراً لكفاءتها العالية وتنوعها. تؤثر هندسة أنبوب التفريغ، وخاصة مساحته المقطعية، بشدة على معاملات البلازما الرئيسية مثل كثافة الإلكترون وكثافة الأيونات ودرجة حرارة الإلكترون، والتي تعمل كمحدد مهم لسلوك البلازما. يتضمن امتصاص الطاقة وتوزيع المجال الكهرومغناطيسي يستخدم هذا العمل برنامج COMSOL Multiphysics للتحقيق في تأثير التغيرات في مساحة المقطع العرضي للأنبوب على خصائص البلازما. والهدف هو تحديد الأنماط من خلال تكوين الأوعية التي يمكن أن تحسن أداء وتصميم الأنظمة القائمة على البلازما، وقد تؤدي إلى تحسينات في تنقية الأنسجة الطبية والمركبات البيئية وفي التصنيع. كانت مساحة المقطع العرضي لأنبوب التفريغ على شكل مستطيل بطول ثابت 25 cm وعرض مختلف  $14 \text{ cm}^{-1}$ . يؤثر تغيير مساحة أنبوب التفريغ  $25-350 \text{ cm}^2$  بشكل كبير على الاستقرار الحراري وتوزيع الطاقة واختراق البلازما. لوحظت تغييرات في درجة الحرارة وكثافة الإلكترون مع زيادة مساحة المقطع العرضي. وجد أن أقصى كثافة إلكترونية  $2.05 \times 10^{18} \text{ m}^{-3}$  عند مساحة مقطع عرضي  $175 \text{ cm}^2$ . بينما تقلبت درجة حرارة الإلكترون من 1.5 إلكترون فولت عند  $A = 100 \text{ cm}^2$  إلى 1.75 إلكترون فولت عند  $A = 25 \text{ cm}^2$  مع أيضاً أقصى قيمة 1.65 إلكترون فولت عند  $A = 175 \text{ cm}^2$ .

**الكلمات المفتاحية:** بلازما، مايكروويف، COMSOL، تفريغ الأرجون، تفريغ المايكروويف.